Al-imad Journal of Humanities and Applied Sciences (AJHAS)
مجلة العماد للعلوم الإنسانية والتطبيقية
ISSN: 3106-0323
Volume 2 – Issue 1 – 2026
Pages 234-242

Angular Dependence of the Total Cross Section in Inverse Compton Scattering (Theoretical Study)

Sana Almabrouk Almahdi *
Department of Physics, Faculty of science Al-Ajaylat, University of Zawia, Libya
*Corresponding: s.almahdi@zu.edu.ly

الاعتماد الزاوي للمقطع العرضي الكلي في استطارة كومبتون العكسية (دراسة نظرية)

سناء المبروك المهدي *
قسم الفيزياء، كلية العلوم العجيلات، جامعة الزاوية، ، ليبيا

Received: 17-12-2025; Accepted: 26-01-2026; Published: 02-03-2026

Abstract:
Inverse Compton Scattering (ICS) of relativistic electrons with low-energy laser photons is a highly efficient mechanism for generating high-energy gamma rays. This study presents a theoretical calculation of the total cross section for ICS in head-on collisions, specifically investigating its dependence on the scattering angle (θ_s). The total cross section is a fundamental parameter for accurately estimating gamma-ray production rates and scattering probabilities. Our findings indicate that angular effects significantly influence the cross-sectional values. Results show that at high gamma-ray energies, the total cross section decreases, whereas at lower energies—corresponding to larger scattering angles—it approaches the classical Thomson scattering limit ($\sigma_{Th\approx}$665mb). This transition confirms the consistency of the theoretical model across different energy regimes. Data from the SLEGS, Hayakawa, and LADON facilities were utilized to verify these angular dependencies. The results demonstrate an inverse relationship between the energy of the produced gamma rays and the scattering probability. These insights are crucial for optimizing ICS-based sources utilized in nuclear physics, medical imaging, and industrial applications, particularly in the transmutation of nuclear waste.

Keywords: Inverse Compton Scattering, total cross section, relativistic electrons, scattering angle, gamma rays.

الملخص
تُعدّ استطارة كومبتون العكسية *(ICS)* للإلكترونات النسبية مع فوتونات الليزر منخفضة الطاقة آلية عالية الكفاءة لتوليد أشعة غاما عالية الطاقة .تقدم هذه الدراسة حساباً نظرياً للمقطع العرضي الكلي لاستطارة كومبتون العكسية في حالة التصادمات الرأسية، مع تقصي اعتماده بشكل محدد على زاوية الاستطارة*(θs)* ويمثل المقطع العرضي الكلي بارامتراً أساسياً للتقدير الدقيق لمعدلات إنتاج أشعة غاما واحتمالية الاستطارة .وتشير نتائجنا إلى أن التأثيرات الزاوية تؤثر بشكل كبير على قيم المقطع العرضي .كما أظهرت النتائج أنه عند طاقات أشعة غاما العالية، يتناقص المقطع العرضي الكلي، بينما عند الطاقات المنخفضة والتي تقابل زوايا استطارة أكبر فإنه يقترب من حد استطارة طومسون الكلاسيكي. *($\sigma_{Th\approx}665mb$)* ويؤكد هذا التحول اتساق

النموذج النظري عبر أنظمة الطاقة المختلفة .وقد تم استخدام بيانات من مرافق *SLEGS* و *Hayakawa* و *LADON*للتحقق من هذه الاعتمادات الزاوية .وتثبت النتائج وجود علاقة عكسية بين طاقة أشعة غاما المنتجة واحتمالية الاستطارة .وتكتسب هذه الرؤى أهمية بالغة لتحسين المصادر القائمة على استطارة كومبتون العكسية المستخدمة في الفيزياء النووية، والتصوير الطبي، والتطبيقات الصناعية، ولا سيما في معالجة النفايات النووية.

الكلمات المفتاحية: استطارة كومبتون العكسية، المقطع العرضي الكلي، إلكترونات نسبية، زاوية الاستطارة، أشعة غاما.

1. Introduction

Inverse Compton Scattering (ICS) represents a sophisticated mechanism wherein a high-energy beam of relativistic electrons interacts with relatively low-energy laser photons. During this interaction, the photons gain significant energy from the electrons, resulting in the emission of high-energy gamma rays (ur Rehman et al., 2015). These produced gamma rays are characterized by exceptional properties, including high intensity, tunable energy levels, quasi-monochromaticity, a narrow angular spread, and high polarization (Taira et al., 2010). Such unique features render ICS-generated beams indispensable for diverse scientific and industrial applications, ranging from polarized positron generation and electron beam diagnostics to fundamental nuclear physics research and non-destructive testing (Taira et al., 2010). Furthermore, this technology demonstrates immense potential in environmental engineering, specifically for the transmutation of radionuclides to facilitate nuclear waste disposal (ur Rehman et al., 2015).

To optimize the efficiency of these applications, it is essential to accurately estimate the gamma-ray yield, which necessitates a precise calculation of the scattering probability. This probability is quantitatively defined by the total cross-section (σ_t), a parameter that is inherently sensitive to the geometric and energetic conditions of the collision. While previous literature has extensively explored how the total cross-section depends on the energy of the incident electrons (Lee et al., 2018; ur Rehman et al., 2016), there is a critical need for a deeper theoretical understanding of its angular behavior.

This study aims to bridge this gap by theoretically investigating the dependence of the total ICS cross-section on the scattering angle (θ_S). A primary objective is to demonstrate that at large scattering angles where the energy transfer is minimized—the cross-section converges toward the classical Thomson scattering limit ($\sigma_{Th}\approx 665mb$).By performing detailed calculations starting from a scattering angle of zero up to large angles, this work elucidates the angular effects that influence the probability of gamma-ray production. Understanding this relationship is vital for the advancement of ICS-based radiation sources and their integration into medical and industrial fields.

2. Inverse Compton Scattering Theory

In the process of Inverse Compton Scattering, high-energy gamma photons are generated through the collision of relativistic electrons and laser photons (Hajima & Fujiwara, 2016). The process is termed "Inverse" because, unlike the standard Compton effect, the photons gain energy from the electrons (Ur, 2015). Essentially, it is the operational opposite of conventional Compton scattering, where electrons typically gain energy at the expense of photons (ur Rehman et al., 2016).

When a low-energy laser photon (E_L) undergoes an elastic collision with a high-energy relativistic electron (E_e) at a specific collision angle (θ_L), its energy increases

dramatically. The photon then undergoes backscattering at a scattering angle (θ_S), a phenomenon often referred to as Compton Backscattering (Fujiwara, 2010). This interaction results in a gamma-ray beam characterized by a pencil-like shape within a narrow cone, where the energy of the resulting gamma ray is denoted by Eγ (D'Angelo et al., 2000; Lee et al., 2018).

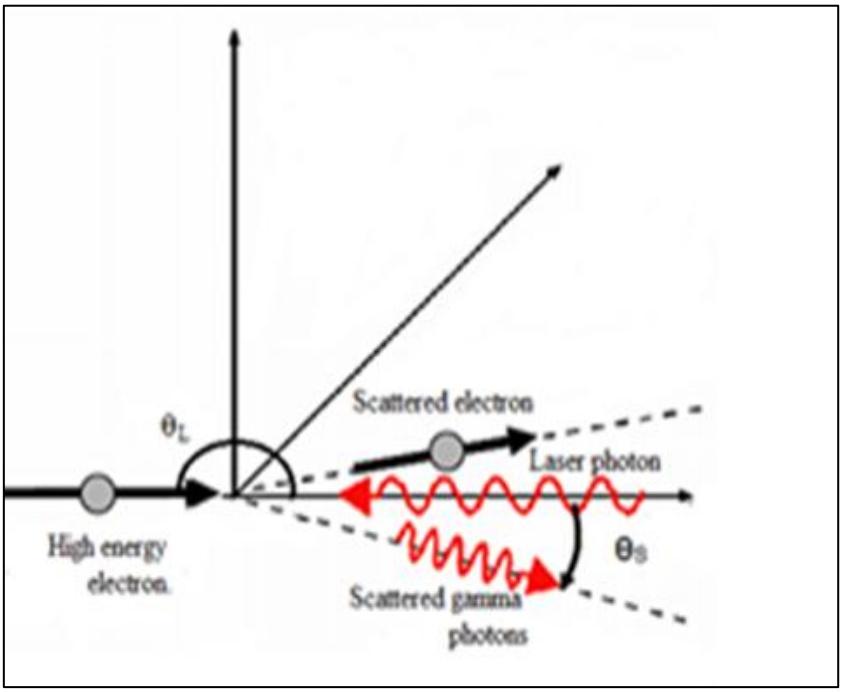

Figure 1: illustrates the schematic diagram of the inverse Compton scattering mechanism in the case of a head-on collision (M. Fujiwara, 2010)

The energy of the gamma rays produced in the case of a head-on collision is given by the following equation Eq (1) (Aoki et al., 2004):

$$E_\gamma = \frac{4\gamma^2 E_L}{1 + (\gamma\theta_S)^2 + \frac{4\gamma E_L}{m_e c^2}} \qquad (1)$$

Where:

E_L is laser photon energy.

γ is Lorentz's constant having a value equal to ($\frac{E_e}{m_e c^2}$), which is the ratio between the kinetic energy of the electron and its rest energy, m_e is electron mass, c is Speed of light in a vacuum.

θ_S is Scattering angle.

1. Total cross section of inverse Compton Scattering

The total cross section of the inverse Compton scattering is given by the integration of the Klein-Nishina equation as follows (Irani et al., 2014):

$$\sigma_t = \int_0^{\theta_c} \frac{d\sigma}{d\Omega}\, d\Omega \qquad (2)$$

Where:
$\frac{d\sigma}{d\Omega}$ is the differential cross-section of Inverse Compton Scattering
$d\Omega$ is a solid angle, and it equal to $sin\ sin\ \theta$ dθ dφ, by substituting into Eq. (2) we obtain:

$$\sigma_t = \int_0^{2\pi} \int_0^{\pi} \frac{d\sigma}{d\Omega}\ sin\ \theta_s\ d\theta_s\ d\varphi \qquad (3)$$

$$\sigma_t = 2\pi \int_0^{\pi} \frac{d\sigma}{d\Omega}\ sin\ \theta_s\ d\theta_s \qquad (4)$$

The differential cross-section of the inverse Compton scattering (angular distribution) $\frac{d\sigma}{d\Omega}$ is given by the Klein-Nishina formula (Irani et al., 2014), (Nishina, Y, 1929):

$$\frac{d\sigma}{d\Omega} = \frac{r_e^2 R^2}{2}\left[R + \frac{1}{R} - 1 + cos^2\theta_s\right] \qquad (5)$$

Where:
r_e is the electron radius**.**
R is the ratio of the photon's energy before and after the collision, and is given by (Irani et al., 2014)**:**

$$R = \frac{1}{1 + \left(\frac{E_\gamma}{m_e c^2}\right)(1 - cos\ \theta_s\ )} \qquad (6)$$

Substituting from Eq. (5) into Eq. (4), we obtain:

$$\sigma_t = \pi r_e^2 R^2 \int_0^{\pi} \left[R + \frac{1}{R} - 1 + cos^2\theta_s\right]\ sin\ \theta_s\ d\theta_s \quad (7)$$

In Eq. (7) if the energy of the gamma rays is less than the rest energy of the electron (R=1), then the total cross section is equal to Thomson cross section scattering (σ_{Th}) (Irani et al., 2014).

$$\sigma_t = \pi r_e^2 \int_0^{\pi} (1 + cos^2\theta_S) sin\ \theta_S\ d\theta_s \qquad (8)$$

$$\sigma_t = \sigma_{Th} = 665\ mb$$

2. Selected facilities

There are many inverse Compton scattering facilities around the world that produce Avery high gamma ray energy (ur Rehman et al., 2016). data from three different facilities were selected: the Shanghai Laser Electron Gamma Source (SLEGS) facility in China (Lee et al., 2018) at the Shanghai Synchrotron Radiation, LADON facility in Italy at the Frascati National Laboratory (D'Angelo et al., 2000) and the proposed facility by Hayakawa (ur Rehman et al., 2016). Table 1 shows the laser and electron energies used in the selected facilities.

Table 1: Data of the facilities selected for the overall cross-section calculations (ur Rehman et al., 2016) , (Lee et al., 2018) , (D'Angelo et al., 2000)

Facility	Electron energy (GeV)	Laser energy(eV)
SLEGS	3.5	0.1165
Hayakawa	0.35	1.156
LADON	1.5	2.45

3. Results and Discussion

By substituting the data shown in Table 1 into the previous equations, we obtained the results for the total cross section values and gamma ray energy values for the Inverse Compton Scattering, shown in Tables 2, 3, and 4 at the SLEGS, Hayakawa, and LADON facilities respectively

Table 2: The resulting values of gamma ray energy and total cross section for inverse Compton scattering at the SLEGS facility.

$\theta_S(mrad)$	$E_\gamma(MeV)$	R	$\sigma_t\ (mb)$
0	21.73	0.02	11
0.25	5.55	0.08	40
0.5	1.72	0.23	103
1	0.46	0.53	244
2	0.21	0.82	456
3	0.12	0.91	552
4	0.05	0.95	597
5	0.03	0.96	620
10	0.02	0.99	653
20	4.66×10^{-3}	1	662
30	1.16×10^{-3}	1	664
40	5.18×10^{-4}	1	664
50	2.91×10^{-4}	1	664
60	1.86×10^{-4}	1	665
70	1.29×10^{-4}	1	665
80	9.51×10^{-5}	1	665
90	7.28×10^{-5}	1	665
100	5.75×10^{-5}	1	665
200	1.29×10^{-5}	1	665

Table 3: The resulting values of gamma ray energy and total cross section for inverse Compton scattering at the Hayakawa facility.

θ_S(mrad)	$E_\gamma(MeV)$	R	σ_t (mb)
0	2.16	0.19	87
0.25	2.09	0.2	89
0.5	1.93	0.21	94
1	1.47	0.26	115
2	0.75	0.4	180
3	0.41	0.55	258
4	0.25	0.67	333
5	0.17	0.75	397
10	0.05	0.92	564

20	0.01	0.98	636
30	0.01	0.99	652
40	$2{,}89\times10^{-3}$	0.99	658
50	1.85×10^{-3}	1	660
100	4.62×10^{-4}	1	664
200	1.16×10^{-4}	1	665
300	5.14×10^{-5}	1	665
400	2.89×10^{-5}	1	665
500	1.85×10^{-5}	1	665
600	1.28×10^{-5}	1	665

Table 4: The resulting values of gamma ray energy and total cross section for inverse Compton scattering at the LADON facility.

θ_S(mrad)	$E_\gamma(MeV)$	R		$\sigma_t(mb)$
0	79.94	0.01		3
0.25	52.99	0.01		5
0.5	26.33	0.02		9
1	8.73	0.06		27
2	2.38	0.18		81
3	1.07	0.32		143
4	0.61	0.46		206
5	0.39	0.57		267
10	0.1	0.84		479
20	0.02	0.95		606
30	0.01	0.98		638
40	3.92×10^{-3}	0.99		649
50	2.72×10^{-3}	0.99		655
60	2.00×10^{-3}	0.99		658
70	1.53×10^{-3}	1		660
80	1.20×10^{-3}	1		661
90	9.80×10^{-4}	1		662
100	2.45×10^{-4}	1		662
200	1.08×10^{-4}	1		664
300	6.13×10^{-5}	1		665
400	3.92×10^{-5}	1		665
500	2.72×10^{-5}	1		665
600	2.00×10^{-5}	1		665
700	1.53×10^{-5}	1		665
800	1.21×10^{-5}	1		665
900	9.80×10^{-6}	1		665
1000	6.13×10^{-6}	1		665

From Tables 2, 3, and 4 we noted that the maximum energy values of gamma rays produced by inverse compton scattering can be obtained when the scattering angle equals to zero; in SLEGS facility the maximum energy is equal to 21.73MeV, in Hayakawa facility is 79.94 MeV, and in LADON facility is 2.16 MeV, also we noted that when the scattering angle increases, the energy of the produced gamma rays decreases while the total cross section increases, and we showed that when the energy of the produced gamma rays becomes less than the rest energy of the electron, then R

=1, and consequently, the total cross-section of inverse Compton scattering approaches or equals the Thomson scattering ($\sigma_t = 665\ mb$).
From the Tables 2, 3 and 4, we can obtain the graph of the angular dependence of the total cross-section in inverse Compton scattering, as shown in the Figures 2, 3, and 4 at the SLEGS, Hayakawa, and LADON facilities respectively.
The Figures 2, 3, and 4 showed that the total cross section graph of the inverse Compton scattering takes the same shape even though the facilities data are different, also showed from the graph that as the scattering angle increases, the total cross section area of the inverse Compton scattering increases, and this continues to increase until it reaches its maximum value, which is Thomson scattering. At this point, the total cross-sectional area will not increase no matter how much the scattering angle increases, and this apply to all facilities worldwide.

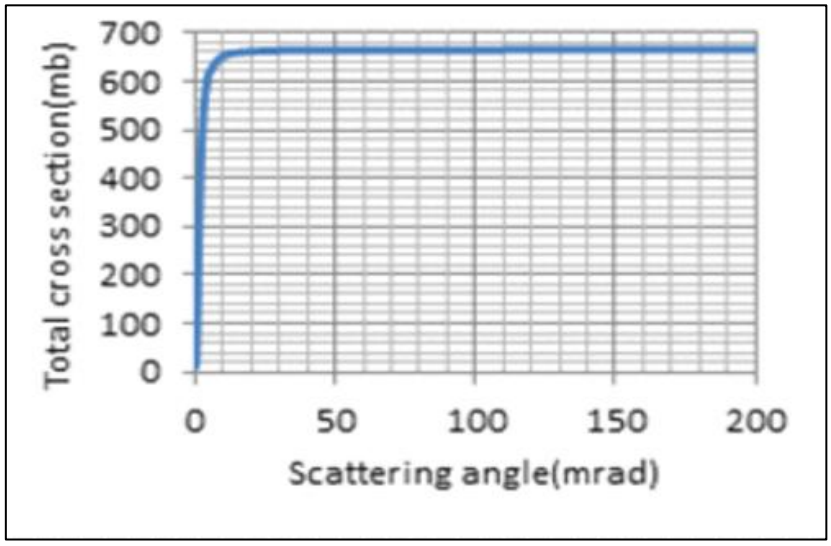

Figure 2: Angular dependence of the total cross-section for inverse Compton scattering at SLEGS facility

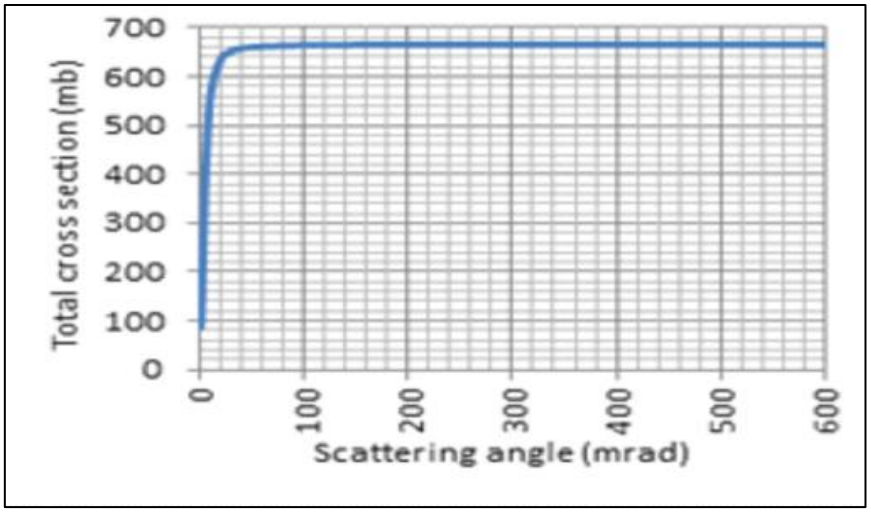

Figure 3: Angular dependence of the total cross-section for inverse Compton scattering at Hayakawa facility.

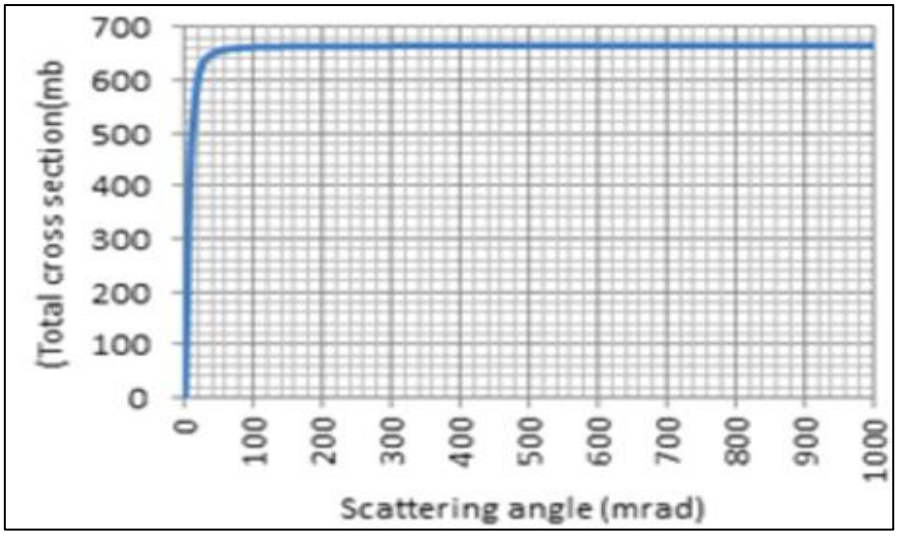

Figure 4: Angular dependence of the total cross-section for inverse Compton scattering at LADON facility

Conclusion

The results showed that the scattering angle significantly affects Compton scattering. At a zero angle, the gamma photon energy is at its highest, while the total cross-sectional area is at its lowest. At larger angles, the photon energy decreases and the cross-sectional area increases, approaching the Thomson limit, thus confirming the findings. An inverse relationship between photon energy and scattering probability was demonstrated, highlighting the importance of the scattering angle dependence of inverse Compton scattering. While previous studies have focused on the electron energy dependence of scattering, this work elucidates the angular effects, providing a more comprehensive understanding of this process.

References

[1] Aoki, K., Hosono, K., Hadame, T., Munenaga, H., Kinoshita, K., Toda, M., Amano, S., Miyamoto, S., Mochizuki, T., Aoki, M., & Li, D. (2004). High-energy photon beam production with laser-Compton backscattering. *Nuclear Instruments and Methods in Physics Research Section A: Accelerators, Spectrometers, Detectors and Associated Equipment*, *516*(2–3), 228–236. https://doi.org/10.1016/j.nima.2003.08.153

[2] D'Angelo, A., Bartalini, O., Bellini, V., Sandri, P. L., Moricciani, D., Nicoletti, L., & Zucchiatti, A. (2000). Generation of Compton backscattering \gamma-ray beams. *Nuclear Instruments and Methods in Physics Research A*, *455*, 1–6.

[3] Fujiwara, M. (2010). *MeV photons from inverse Compton scattering and applications for science* [Workshop presentation]. Saskatoon workshop.

[4] Hajima, R., & Fujiwara, M. (2016). Narrow-band GeV photons generated from an x-ray free-electron laser oscillator. *Physical Review Accelerators and Beams*, *19*(2), 020702 . https://doi.org/10.1103/PhysRevAccelBeams.19.020702

[5] Irani, E., Omidvar, H., & Sadighi-Bonabi, R. (2014). Gamma rays transmutation of Palladium by bremsstrahlung and laser inverse Compton scattering. *Energy Conversion and Management*, *77*, 558–563. https://doi.org/10.1016/j.enconman.2013.09.029

[6] Lee, J., Rehman, H. U., & Kim, Y. (2018). A feasibility study on the transmutation of ^{100}Mo to ^{99m}Tc with Laser-Compton scattering photons.

Nuclear Technology, *201*(1), 41–51 . https://doi.org/10.1080/00295450.2017.1392397
[7] Nishina, Y. (1929). Über die Streuung von Strahlung durch freie Elektronen nach der neuen relativistischen Quantendynamik von Dirac. *Zeitschrift für Physik*, *52*, 853–868 . https://doi.org/10.1007/BF01366453
[8] Taira, Y., Adachi, M., Zen, H., Katoh, M., Yamamoto, N., Hosaka, M., Takashima, Y., Soda, K., & Tanikawa, T. (2010). Generation of ultra-short gamma-ray pulses by laser Compton scattering in an electron storage ring. *Proceedings of IPAC10*, 2117–2119.
[9] Ur, C. A. (2015). Gamma beam system at ELI-NP. *AIP Conference Proceedings*, *1645*, 237–245 . https://doi.org/10.1063/1.4909580
[10] ur Rehman, H., Lee, J., & Kim, Y. (2015). *A comparison of laser-induced bremsstrahlung and laser Compton scattering for (\γ, n) photo-transmutation of hazardous nuclear waste* [Paper presentation]. Transactions of the Korean Nuclear Society Autumn Meeting.
[11] ur Rehman, H., Lee, J., & Kim, Y. (2016). Use of quasi-monoenergetic laser Compton scattering beam for enhanced transmutation of nuclear waste. *Journal of Nuclear Science and Technology*, *53*(8), 1132–1141. https://doi.org/10.1080/00223131.2015.1091751

